Tuning Nanostructure Morphology and Gold Nanoparticle "Locking" of Multi-Responsive Amphiphilic Diblock Copolymers†

Adam E. Smith,‡ Xuewei Xu,‡ Thomas U. Abell,‡ Stacey E. Kirkland,‡ Ryan M. Hensarling,‡ and Charles L. McCormick*,‡,§

Department of Polymer Science and Department of Chemistry and Biochemistry, The University of Southern Mississippi, Hattiesburg, Mississippi 39406

Received December 19, 2008; Revised Manuscript Received February 9, 2009

ABSTRACT: Reversible addition-fragmentation chain transfer (RAFT) polymerization was utilized to prepare multiresponsive, self-assembling amphiphilic poly[(*N*,*N*-dimethylaminoethyl methacrylate)$_x$-*b*-(*N*-isopropylacrylamide)$_y$] (DMAEMA$_x$-*b*-NIPAM$_y$). Controlling block lengths, solution pH, and NaCl concentration to elicit changes in the hydrophilic mass fraction resulted in specific morphological changes upon thermally induced assembly. At $y = 102$ (68 wt % DMAEMA), DMAEMA$_{165}$-*b*-NIPAM$_{102}$ copolymers self-assemble into simple core−shell micelles (58 nm). Increasing y to 202 (48 wt % DMAEMA) leads to a mixture of spherical micelles (78 nm) and worm-like micelles ($D = 50-100$ nm, $L = 400-500$ nm). Further increasing y to 435 (36 wt % DMAEMA) produces vesicular structures (179 nm). Significantly, reversible assembly of these nanostructures from the present stimuli-responsive diblock copolymers can be accomplished directly in aqueous media without the necessity of dialysis or manipulation with cosolvents. Additionally, the associated nanostructures can be shell cross-linked above the critical aggregation temperature *via* the *in situ* formation of gold nanoparticles yielding assemblies with long-term aqueous stability.

Introduction

The ability of amphiphilic block copolymers to self-assemble into various morphologies in aqueous solution in response to specific stimuli has attracted widespread interest for potential applications as targeted drug delivery and diagnostic vehicles.[1−13] For example, assembly into spherical micelles, cylindrical micelles, and vesicles among others has been observed.[14−16] The self-assembled morphology of amphiphilic block copolymers is largely influenced by the relative hydrophilic dimensions of the hydrophobic and hydrophilic blocks.[17] Discher and Ahmed related the assembled morphology to the hydrophilic mass fraction, *f*, with a value greater than 50% leading to micelles, between 40 and 50% yielding cylindrical or worm-like micelles, and 35 ± 10% giving rise to vesicles or polymersomes.[18] In addition to the ratio of the hydrophilic and hydrophobic block lengths, a number of factors including the concentration of the polymer and ionic strength of the solution have been shown to influence the resulting aggregate morphology.[19−21]

Stimuli-responsive block copolymers afford a facile method for tuning the hydrophilic mass fraction to provide access to various solution morphologies. Such "smart" materials exhibit dramatic changes in properties in response to the alteration of external stimuli, such as temperature, pH, and ionic strength.[22−27] A number of investigations have documented reversible switching between morphologies by tuning the hydrophilic to hydrophobic ratio with changes in pH[28−31] and temperature.[32−34] Systems responsive to two stimuli provide an even greater level of control and are of immense importance for biologically relevant applications.[35] Examples of dually responsive systems include poly(propylene oxide-*b*-*N*,*N*-diethylaminoethyl methacrylate) reported by the Armes group[36] and the poly(*N*-isopropylacrylamide)-*b*-poly(acrylic acid) (NIPAM-*b*-AA) reported by Mueller and co-workers[37] and Nuopponen and Tenhu.[38] Certain homopolymers also display such dual responsiveness. For example, poly(*N*,*N*-dimethylaminoethyl methacrylate) (PDMAEMA) is both thermo- and pH-responsive.[39−41]

The delivery of drugs from nanostructured assemblies derived from block copolymers has been extensively studied in recent years. However, despite the recognized potential as drug delivery vehicles, self-assembling structures are inherently limited due to multimer dissociation upon injection into the bloodstream. These amphiphilic aggregates experience a large dilution effect which leads to concentrations below the critical aggregation concentration and eventually burst release of the drug payload.[42] This can be avoided by cross-linking the nanostructure. Unfortunately, the core cross-linking often decreases drug carrying capacity and thus hinders application as a drug delivery vehicle.[43] An alternative approach is to cross-link the shell of the self-assembled aggregate. The first example of shell cross-linked (SCL) micelles was reported by Wooley and co-workers, who oligomerized pendant styrene groups using free radical chemistry.[44] Numerous strategies have since been developed for the shell cross-linking of micelles including the following: carbodiimide coupling;[13,45−47] covalent cross-linking with 1,2-bis(2-iodoethoxy)ethane,[48−50] divinyl sulfone,[51] or glutaraldehyde;[26] interpolyelectrolyte complexation;[24,52−54] metal-catalyzed cross-linking;[55] and click chemistry.[56] Our group recently developed a shell cross-linking method which utilizes a facile reaction between activated esters and primary amines to prepare SCL micelles and reversible SCL micelles.[57,58] For a thorough review of shell cross-linked micelles, the reader is referred to a recent publication by Read and Armes.[59]

Gold nanoparticles (AuNPs) have been the focus of intense research over the past decade due to their unique properties and potential application in many areas including biomedical materials, optics, and electronics.[60] Thiol chemistry has widely been used to modify the surface of AuNPs with synthetic polymers[61−64] and biomacromolecules.[65−67] Conventional reducing agents such as $NaBH_4$ are used to produce zerovalent AuNPs in the presence of thiolated stabilizing agents. Recently, there have been numerous reports utilizing amine-containing copoly-

† Paper No. 138 in a series on Water Soluble Polymers.

* To whom correspondence should be addressed. E-mail: Charles.McCormick@usm.edu.

‡ Department of Polymer Science.

§ Department of Chemistry & Biochemistry.

10.1021/ma802827p CCC: $40.75
Published on Web 03/24/2009

Scheme 1. Preparation of Multi-Responsive DMAEMA-*b*-NIPAM Block Copolymers via RAFT Polymerization

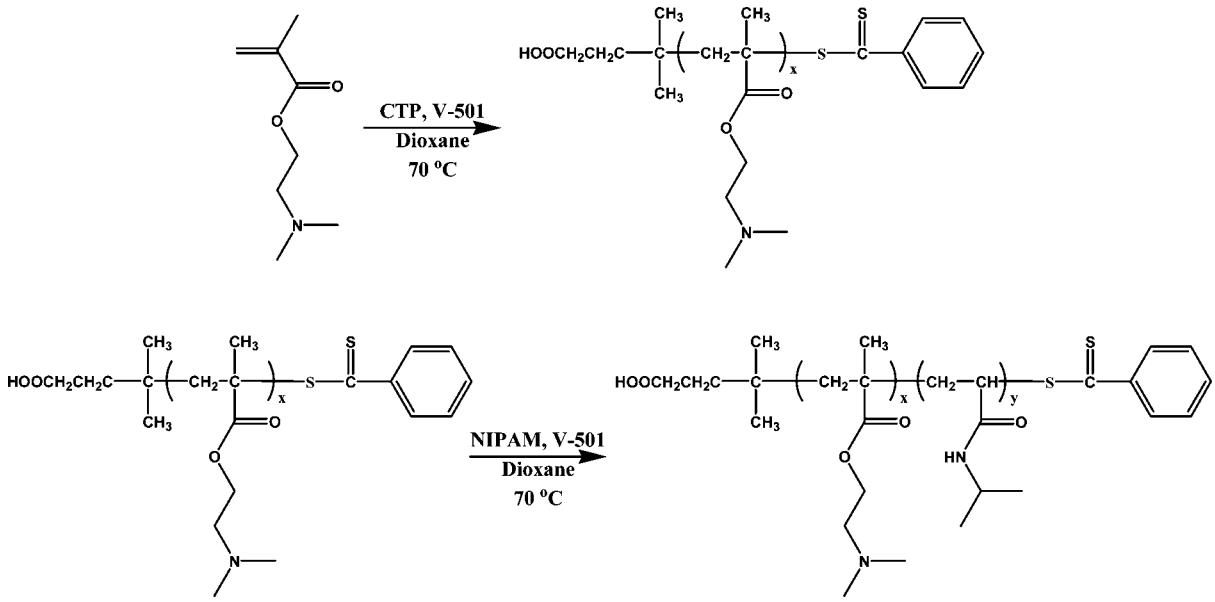

mers that can act as both a reducing agent and a stabilizing agent.[64,68−71] Ishii and co-workers reported the synthesis of biotin-functionalized PEGylated gold nanoparticles using a PDMAEMA block to reduce $AuCl_4^-$ to zerovalent AuNPs.[71] Armes and co-workers recently reported the synthesis of poly-(2-(methacryloyloxy)ethyl phosphorylcholine)-coated AuNPs also using PDMAEMA as a reducing block.[64] Building on these previous reports as well as our experience in the arena of shell cross-linked micelles and vesicles,[24,52,54,57,58] we recently synthesized AuNP-decorated vesicles derived from a stimuli-responsive block copolymer, $DMAEMA_{73}$-*b*-$NIPAM_{99}$, synthesized by RAFT polymerization.[72] Above the LCST, the block copolymer self-assembles into vesicles and can be subsequently cross-linked by the *in situ* reduction of $NaAuCl_4$ to AuNPs by the PDMAEMA.

Herein, we report the synthesis of a series of DMAEMA-*b*-NIPAM block copolymers utilizing reversible addition-fragmentation chain transfer (RAFT) polymerization. RAFT provides a facile method of preparing the desired block copolymer architecture while maintaining precise control over the macromolecular characteristics (molecular weight, copolymer composition, functionality, etc.) that dictate nanostructure morphology.[73−76] The block lengths were varied to give hydrophilic mass fractions necessary for the formation of micelles, worm-like micelles, and vesicles above the LCST.[18] Additionally, polymer concentration, pH, and ionic strength have been varied to determine their respective effects on the resulting assembled morphology. The nanostructures were subsequently cross-linked by the *in situ* reduction of $NaAuCl_4$ to AuNPs within the PDMAEMA layer and studied using dynamic light scattering (DLS) and transmission electron microscopy (TEM). It is important to note that metal cross-linking allows not only facile

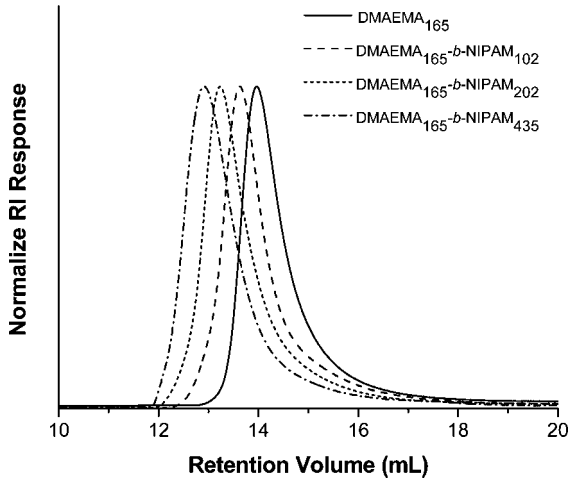

Figure 1. SEC chromatograms for the chain extension of $DMAEMA_{165}$ macroCTA to yield three $DMAEMA_{165}$-*b*-$NIPAM_y$ block copolymers using reversible addition-fragmentation chain transfer polymerization.

Table 1. Summary of DMAEMA-*b*-NIPAM Block Copolymer Series Molecular Weight and Composition

polymer	M_n[a]	PDI[a]	hydrophilic mass fraction (%) at 50 °C, pH 5[b]
$DMAEMA_{165}$	26 200	1.04	100
$DMAEMA_{165}$-*b*-$NIPAM_{102}$	37 700	1.10	70
$DMAEMA_{165}$-*b*-$NIPAM_{202}$	49 000	1.17	53
$DMAEMA_{165}$-*b*-$NIPAM_{435}$	75 400	1.17	35

[a] As determined by SEC. [b] Determined by ^1H NMR in D_2O.

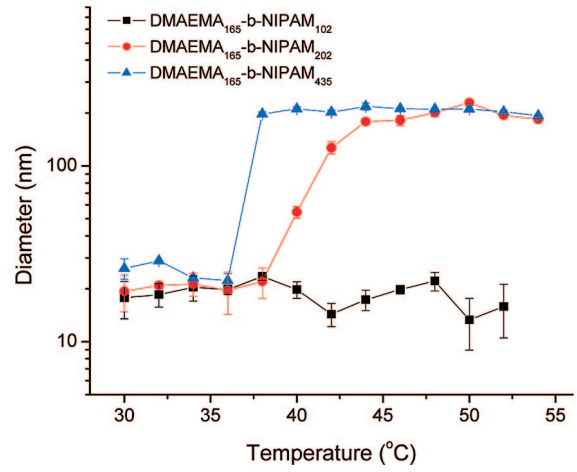

Figure 2. Hydrodynamic diameter vs temperature data for the three $DMAEMA_{165}$-*b*-$NIPAM_y$ block copolymers showing the effect of block copolymer composition on the self-assembly behavior in aqueous solution (0.01% (w/w) concentration, pH 5.0).

Table 2. Hydrodynamic Diameters Measured from DLS for Block Copolymer Solutions (0.01 wt %) at 50 °C under Varying pH and NaCl Concentrations

	[NaCl] = 0 mM			[NaCl] = 50 mM			[NaCl] = 200 mM		
	solution pH = 5	solution pH = 7	solution pH = 9	solution pH = 5	solution pH = 7	solution pH = 9	solution pH = 5	solution pH = 7	solution pH = 9
$DMAEMA_{165}$-*b*-$NIPAM_{102}$	13.3 ± 4.3	246 ± 7.8	570 ± 10.2	13.3 ± 3.2	16.2 ± 3.3	3010 ± 198	65.1 ± 9.3	71.2 ± 3.9	3730 ± 51.5
$DMAEMA_{165}$-*b*-$NIPAM_{202}$	232 ± 6.6	276 ± 5.3 (66%)	643 ± 14.6	94.1 ± 2.7	112 ± 1.8	3170 ± 364 (83%)	59.9 ± 3.1	58.1 ± 0.7	255 ± 6.6 (58%)
		61.3 ± 2.8 (34%)			181 ± 10.6 (16%)				52.2 ± 3.9 (42%)
$DMAEMA_{165}$-*b*-$NIPAM_{435}$	210 ± 0.6	179 ± 1.6	3250 ± 89.5	108 ± 1.2	261 ± 15.8 (45%)	3760 ± 103	96.1 ± 1.3	88.4 ± 1.0	2000 ± 60.5
					101 ± 8.0 (55%)				

nanostructure "locking" but yields dispersed nanostructures with long-term stability in water.

Experimental Section

Materials. All chemicals were purchased from Aldrich at the highest available purity and were used as received unless otherwise noted. NIPAM (97%, Aldrich) was recrystallized twice from hexane. DMAEMA was dried with CaH_2 and vacuum distilled prior to use. 4,4-Azobis(4-cyanopentanoic acid) (V-501) was donated by Wako Chemicals and was recrystallized twice from methanol. 4-Cyanopentanoic acid dithiobenzoate (CTP) was prepared as previously reported.[77]

General Procedure for the RAFT Polymerization of DMAEMA. A PDMAEMA macroCTA was synthesized according to a previously published procedure.[72] A solution of CTP (88.5 mg, 0.317 mmol), DMAEMA (20.00 g, 127 mmol), and V-501 (17.7 mg, 0.063 mmol) in 31.9 mL of dioxane were added to a 100 mL ampule. The solution was sparged with nitrogen for approximately 30 min and the ampule was placed in a preheated oil bath at 70 °C. The reaction was terminated after 12 h by cooling the reaction tube in an ice bath followed by exposure to air. The product was purified by precipitation into heptanes (3×) and dried under vacuum overnight.

Block Copolymer Synthesis. DMAEMA-*b*-NIPAM block copolymers were synthesized according to a previously published literature procedure.[72] For example, NIPAM (0.80 g, 7.07 mmol), $DMAEMA_{165}$ (0.80 g), and V-501 (1.63 mg, 0.0058 mmol) were dissolved in 4.8 mL of dioxane and added to a 10 mL ampule. After sparging with nitrogen for 30 min, the reaction was allowed to proceed at 70 °C for 3 h. The reaction mixture was then quenched by cooling the reaction vessel in an ice bath and exposure to air. The product was purified by precipitation in hexanes (3×), dissolved in water, and isolated by lyophilization.

Size Exclusion Chromatography (SEC). Homopolymers of DMAEMA were analyzed directly by aqueous size exclusion chromatography (ASEC) using an aqueous eluent of 1.0 wt % acetic acid/0.1 M Na_2SO_4. A flow rate of 0.25 mL/min, Eprogen Inc. columns [CATSEC1000 (7 μ, 50 × 4.6), CATSEC100 (5 μ, 250 × 4.6), CATSEC1000 (7 μ, 250 × 4.6) and CATSEC300 (5 μ, 250 × 4.6)], a Wyatt Dawn EOS multiangle laser light scattering detector (λ = 690 nm), and an Optilab DSP interferometric refractometer (λ = 690 nm) were used. Wyatt DNDC for Windows was used for the PDMAEMA d*n*/dc determination. SEC was used to determine the number-average molecular weight (M_n) and polydispersity indices (PDIs) for the PDMAEMA homopolymer and the block copolymers of DMAEMA and NIPAM. A DMF eluent (0.02 M LiBr) was used at a flowrate of 1.0 mL/min in combination with Viscotek I-Series Mixed Bed low-MW and mid-MW columns, and a Viscotek-TDA 302 (RI, viscosity, 7 mW 90° and 7° true low angle light scattering detectors (670 nm)) at 60 °C. The d*n*/d*c* of each (co)polymer was determined in DMF at 60 °C using a Viscotek refractometer and Omnisec software.

^{1}H NMR Spectroscopy. ^{1}H NMR measurements were performed with a temperature-controlled Varian UNITY INOVA spectrometer operating at a frequency of 499.8 MHz. Samples were prepared in D_2O (HOD internal standard) and spectra were attained for each copolymer at 5 °C increments from 25 to 50 °C. Block copolymer compositions were determined by comparing resonances of the

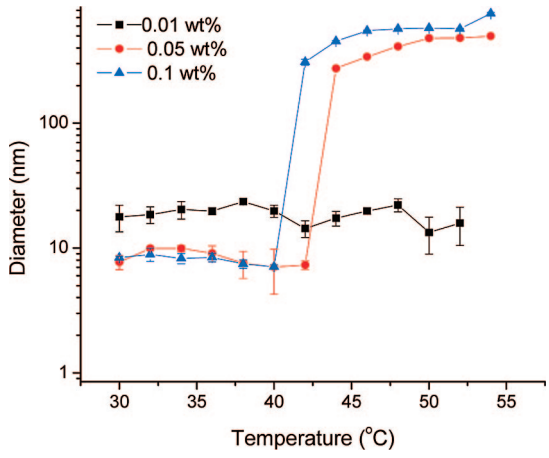

Figure 3. Effect of block copolymer concentration on the temperature-responsive aggregation of $DMAEMA_{165}$-*b*-$NIPAM_{102}$ in aqueous solution (pH 5.0).

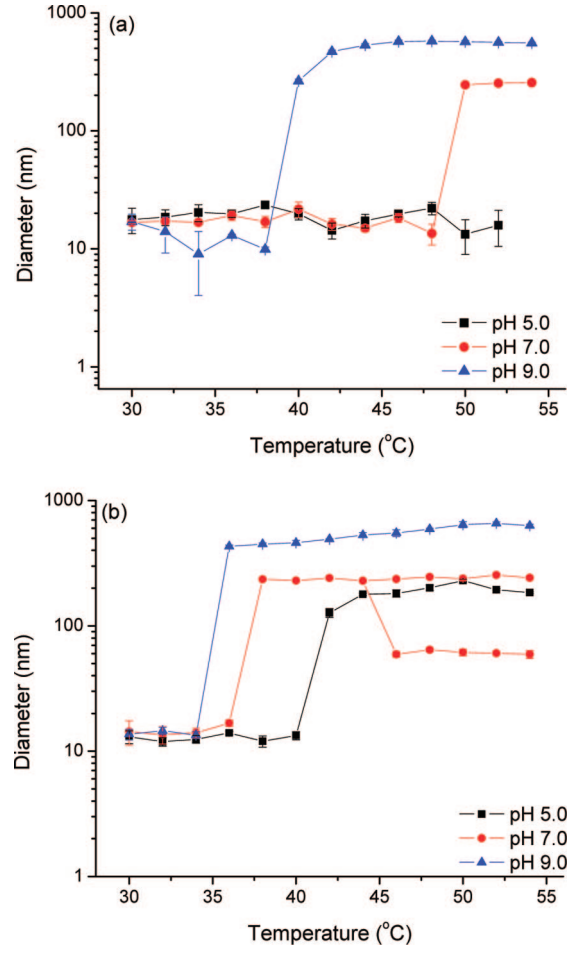

Figure 4. Variation of hydrodynamic diameter with temperature of (a) $DMAEMA_{165}$-*b*-$NIPAM_{102}$ and (b) $DMAEMA_{165}$-*b*-$NIPAM_{202}$ in aqueous solutions (0.01% (w/w)) of varying pH.

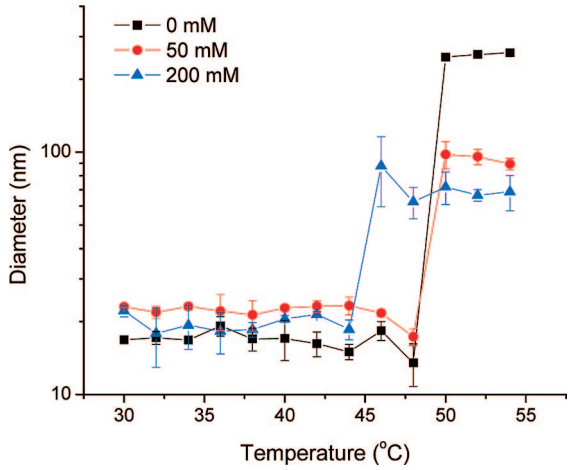

Figure 5. Variation of hydrodynamic diameter with temperature of $DMAEMA_{165}$-*b*-$NIPAM_{102}$ in aqueous solution (0.01 wt %, pH 7.0) at varying NaCl concentration.

PDMAEMA block to those associated with the PNIPAM block in the spectra recorded at 25 °C.

Preparation of Self-Assembled Nanostructures. Copolymers were dissolved directly in HPLC grade water containing 0, 50, or 200 mM NaCl at concentrations varying between 0.01 (0.1 mg/mL) and 0.1 wt % (1.0 mg/mL). The pH was subsequently adjusted to 5, 7, or 9 using 0.1 N HCl or NaOH. Self-assembly of the block copolymers was then induced by increasing the temperature above the critical aggregation temperature (CAT) of the block copolymer.

Gold Nanoparticle Cross-Linking of the Nanostructures. The DMAEMA-*b*-NIPAM copolymer solutions of varying copolymer concentration, pH, and salt concentration were heated to 50 °C (1.0 °C/min) to induce self-assembly. After 30 min, 2−5 μL of a preheated solution of sodium tetrachloroaurate(III) dihydrate solution ($NaAuCl_4$) at pH 6.5 was added to the copolymer solution at 50 °C to give a DMAEMA to Au ratio of 10 to 1 as discussed in previous work.[72] The mixed solution was allowed to stir at 50 °C for 48 h prior to being cooled to room temperature for analysis.

Dynamic Light Scattering. Aqueous block copolymer solution studies were conducted using a Malvern Instruments Zetasizer Nano series instrument equipped with a 4 mW He−Ne laser operating at $\lambda = 632.8$ nm, an avalanche photodiode detector with high quantum efficiency, and an ALV/LSE-5003 multiple τ digital correlator electronics system. Dispersion Technology Software 5.03 (Malvern Instruments) was used to record and analyze the data.

Transmission Electron Microscopy. Transmission electron microscopy measurements were conducted using a JEOL JEM-2100 electron microscope at an accelerating voltage of 200 kV. The specimens were prepared by placing a 5 μL drop of the gold nanoparticle cross-linked nanostructure solution on a carbon-coated copper grid followed by water evaporation at 25 °C.

Results and Discussion

Multi-Responsive DMAEMA-*b*-NIPAM Block Copolymers. $DMAEMA_x$-*b*-$NIPAM_y$ diblock copolymers were synthesized according to Scheme 1. DMAEMA was first polymerized using CTP and V-501 in dioxane to produce a PDMAEMA macroCTA. Monomer conversion was kept below 70% in order to maintain the dithioester chain-end functionality for efficient polymerization of the subsequent PNIPAM block. The PDMAEMA macroCTA ($x = 165$) had M_n and PDI values of 26 200 g/mol and 1.04, respectively. This macroCTA of $DMAEMA_{165}$ was chain extended with NIPAM to give three block copolymers with respective y values of 102, 202, and 435. SEC chromatograms of the copolymer series are shown in Figure 1. All of the SEC traces are unimodal and the PDIs are low (<1.2) indicating near-quantitative blocking efficiency and controlled polymerization. Low molecular weight tailing of the SEC chromatograms is due to the interaction of the PDMAEMA block with the GPC columns used for the analysis of the block copolymer system. Analysis of the PDMAEMA macroCTA via ASEC utilizing CATSEC columns specifically tailored for cationic polymers (but not appropriate for PNIPAM) shows a narrow peak with no perceptible tailing at higher elution volumes (Supporting Information, Figure S1). The molecular weight and composition data of the diblock copolymer series are summarized in Table 1.

Temperature-Induced Assembly: Effect of Polymer Composition. RAFT provides a facile technique for preparing a well-defined series of amphiphilic diblock copolymers of preselected compositions which can be utilized to assess the importance of block lengths on the temperature-responsive assembly. Specific copolymer compositions were targeted to produce hydrophilic mass fractions corresponding to spherical micelles, worm-like micelles, and vesicles as predicted by Discher and co-workers for amphiphilic block copolymers with a permanently hydrophobic block.[18]

Examining the temperature-responsive self-assembly at 0.01 wt % and a pH of 5.0 for the three block copolymers utilizing dynamic light scattering (DLS) reveals a strong dependence of the aggregation behavior on the length of the PNIPAM block. As shown in Figure 2, the copolymer with the shortest NIPAM block, $DMAEMA_{165}$-*b*-$NIPAM_{102}$, does not display a critical aggregation temperature (CAT) and remains dispersed as unimers over the temperature range studied. Increasing the degree of polymerization (DP) of the hydrophobic block from 102 to 202 results in the onset of aggregation at 38 °C and aggregates of hydrodynamic diameter values of ≈220 nm above 44 °C. Further increasing the DP of the PNIPAM block to 435 lowers the CAT to 36 °C while maintaining aggregate sizes of 210 nm above 36 °C. The DLS results are summarized in Table 2.

Temperature-Induced Assembly: Effect of Copolymer Concentration. The size of the aggregates is also strongly influenced by the copolymer concentration. Figure 3 shows the effect of increasing concentration of $DMAEMA_{165}$-*b*-$NIPAM_{102}$ on the unimer-to-nanostructure transition at pH 5.0. As discussed above, at a copolymer concentration of 0.01 wt % (0.1 mg/mL), the copolymer does not undergo a thermally induced transition from unimers to macromolecular aggregates. This can be attributed to the concentration being below the critical aggregation concentration (CAC). Increasing the copolymer concentration to 0.05 wt % (0.5 mg/mL) leads to the onset of

Scheme 2. Idealized Formation of Gold Cross-Linked Nanostructures Formed from the Temperature-Induced Self-Assembly of DMAEMA-*b*-NIPAM Block Copolymers

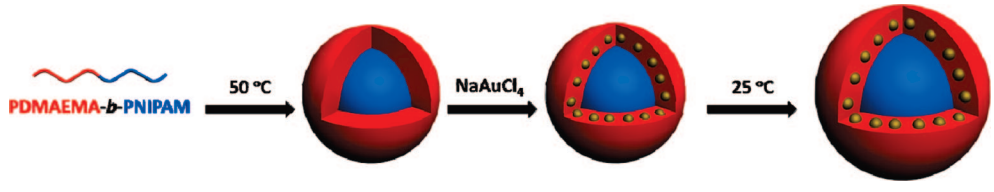

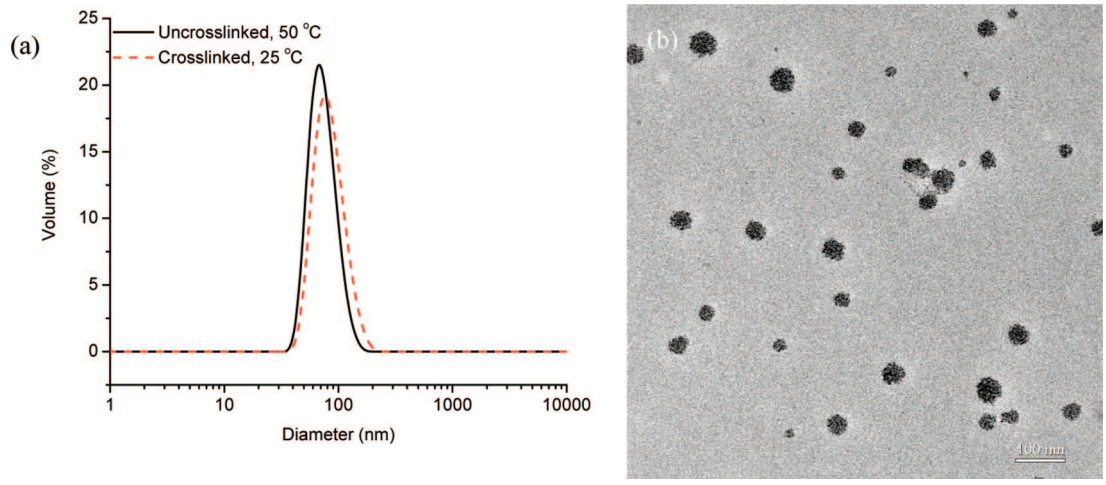

Figure 6. (a) Dynamic light scattering of micelles formed from aqueous solution (0.01 wt %, pH 7.0, 200 mM NaCl) of $DMAEMA_{165}$-*b*-$NIPAM_{102}$ before and after cross-linking. (b) TEM micrograph of AuNP cross-linked $DMAEMA_{165}$-*b*-$NIPAM_{102}$ micelles.

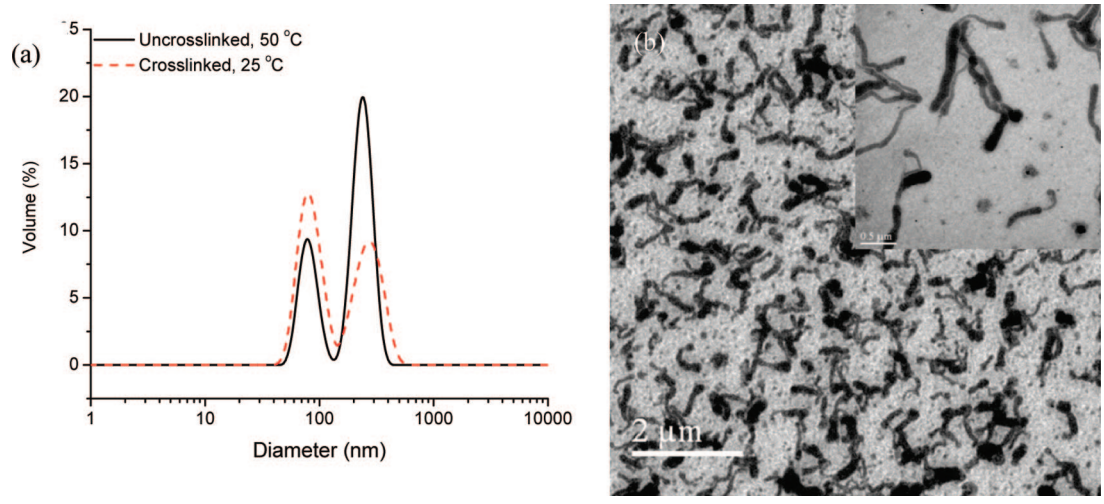

Figure 7. (a) Dynamic light scattering of spherical and worm-like micelles formed from aqueous solution (0.01 wt %, pH 7.0) of $DMAEMA_{165}$-*b*-$NIPAM_{202}$ before and after cross-linking. (b) TEM micrograph of AuNP cross-linked $DMAEMA_{165}$-*b*-$NIPAM_{202}$ spherical and worm-like micelles.

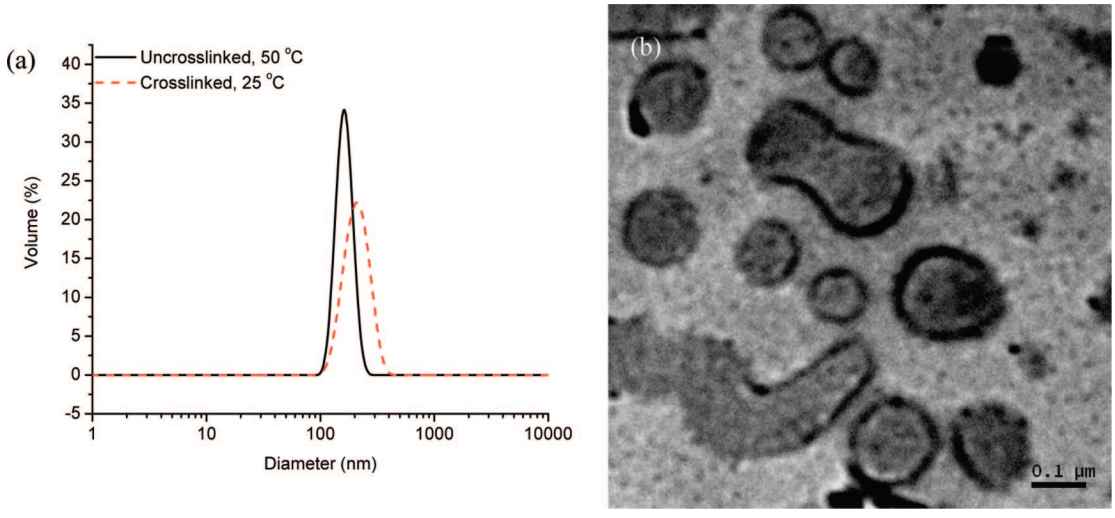

Figure 8. (a) Dynamic light scattering of vesicles formed from aqueous solution (0.01 wt %, pH 7.0) of $DMAEMA_{165}$-*b*-$NIPAM_{435}$ before and after cross-linking. (b) TEM micrograph of AuNP cross-linked $DMAEMA_{165}$-*b*-$NIPAM_{435}$ vesicles.

aggregation at 44 °C and 480 nm nanostructures above 50 °C. Above the CAC, the size of the polymeric aggregates and the CAT show a marked dependence on the copolymer concentration. Further increasing the concentration to 0.1 wt % (1.0 mg/mL) decreases the onset of aggregation to 42 °C and leads to aggregates of 580 nm above 46 °C.

Temperature-Induced Assembly: Effect of pH. The DMAEMA repeat units that comprise the hydrophilic stabilizing blocks are tertiary amines which can be reversibly protonated by adjusting the pH of the solution. Due to the complex stimuli-responsive behavior of the PDMAEMA stabilizing block, altering the pH should have a dramatic effect on the solution aggregation behavior of the block copolymers. Previous studies have reported a strong effect by chain ends and comonomers on the LCST of PNIPAM.[78,79] As the pH of the copolymer solution is increased, the hydrophilicity of the PDMAEMA stabilizing block decreases. At pH 5, the DMAEMA moieties (pK_a 7.3) are 99% protonated which increases the hydrophilicity of the block copolymer so that DMAEMA$_{165}$-*b*-NIPAM$_{102}$ does not possess sufficient hydrophobic character for aggregation in the temperature range of this study at a concentration of 0.01 wt % (Figure 4a). At pH 7, the DMAEMA units are $\sim$ 65% ionized, leading to copolymer aggregates with hydrodynamic diameters of 246 nm above 50 °C. Further increasing the pH to 9.0 decreases the ionization of the PDMAEMA to approximately 2%. This greatly decreases the hydrophilicity of the copolymer system lowering the CAT to 38 °C. Additionally, due to the deprotonation of most of the DMAEMA units, the PDMAEMA block becomes temperature-responsive in the range of this study. At this pH, the aggregates increase in size to 570 nm.

Interestingly, this behavior is not observed for DMAEMA$_{165}$-*b*-NIPAM$_{202}$. Figure 4b shows the effect of pH on the temperature-induced aggregation of 0.01 wt % solutions. At pH values of 5.0 and 9.0, the aggregation behavior of DMAEMA$_{165}$-*b*-NIPAM$_{202}$ follows the expected trends discussed above. At pH 7.0, however, two distinct populations arise above 46 °C. One population has a size slightly larger than the aggregates formed at pH 5.0 ($\sim$240 nm). The smaller-sized population has a hydrodynamic diameter of approximately 60 nm. This mixed population system will be discussed in further detail in a subsequent section.

Temperature-Induced Assembly: Effect of Salt Concentration. Since the PDMAEMA block is a polyelectrolyte, the addition of salt should screen the cationic charges along the polymeric backbone, decreasing the rigidity and subsequently affecting the packing behavior in polymeric aggregates above the CAT of the DMAEMA-*b*-NIPAM copolymers. The addition of NaCl should also have a "salting out" effect on the NIPAM block that would lower the CAT value. Figure 5 shows the effect that addition of salt has on the aggregates formed from DMAEMA$_{165}$-*b*-NIPAM$_{102}$ at a concentration of 0.01 wt % and a solution pH of 7.0. As discussed earlier, in the absence of salt, the block copolymer forms aggregates of 232 nm. When the copolymer is dissolved in an aqueous 50 mM NaCl solution, the size of the aggregates decreases to 94 nm, but the CAT is unchanged. Increasing the NaCl concentration to 200 mM leads to a further decrease in the aggregate size to 60 nm and also decreases the CAT by 4 °C.

AuNP Cross-linking of Assembled Nanostructures. The cross-linking of the self-assembled nanostructures by the *in situ* formation of AuNPs was accomplished using a procedure modified from our previous work according to Scheme 2.[72] The block copolymer solutions were heated to 50 °C at a rate of 1 °C/min and allowed to stir for 30 min prior to the addition of the $NaAuCl_4$. A small volume (2−5 μL) of a $NaAuCl_4$ solution was then added to give a DMAEMA:Au ratio of 10:1. A higher ratio results in incomplete cross-linking while a lower ratio leads to precipitation of the AuNPs in some samples. The AuNP-cross-linking provides a facile method to "lock" the self-assembled nanostructures and further investigate the morphologies of the aggregates studied by DLS. The cross-linked structures are easily analyzed by TEM since the AuNPs act as a staining agent for the nanostructures.

Comparison of DLS and TEM. Figure 6 shows the size distribution determined from DLS and the corresponding TEM images of the AuNP cross-linked aggregates formed from a solution of DMAEMA$_{165}$-*b*-NIPAM$_{102}$ dissolved in 200 mM NaCl at a pH of 7.0. Prior to cross-linking, the aggregates possessed average hydrodynamic diameters of 58 nm at 50 °C. After the cross-linking reaction, the solution temperature was lowered below the CAT to ambient temperature and the aggregate sizes increased to 72 nm. This increase in size is attributed to the rehydration of the PNIPAM core. In the TEM micrographs spherical particles ranging from 30 to 80 nm are observed. From the sizes determined by DLS and TEM, one can conclude that under these conditions DMAEMA$_{165}$-*b*-NIPAM$_{102}$ polymers form a simple core−shell micelle morphology as predicted based on the hydrophilic mass fraction (f = 68%) of this copolymer.[18]

As discussed earlier, when a pH 7.0 solution of DMAEMA$_{165}$-*b*-NIPAM$_{202}$ is heated to 50 °C, Contin analysis of DLS data reveals two distinct populations. Before cross-linking two distributions appear at 61 and 237 nm. After cross-linking, both shift to larger hydrodynamic diameters, 78 and 289 nm, respectively. TEM (Figure 7) provides additional evidence for two populations. The smaller sized distribution arises from spherical micelles while the larger size is attributed to the worm-like structures. These elongated structures have lengths approaching 500 nm with diameters ranging from 50 to 100 nm. The presence of two coexisting morphologies is not surprising and has been reported previously.[18] Significantly, the hydrophilic mass fraction of this system (48 wt %) corresponds to the numbers proposed for the formation of worm-like structures.[18]

When a 0.01 wt % aqueous solution (pH 7.0) of DMAEMA$_{165}$-*b*-NIPAM$_{435}$ is heated to 50 °C, nanostructures of 179 nm are formed as determined from DLS. After *in situ* gold nanoparticle formation to cross-link the aggregates, the apparent hydrodynamic diameters increase to 210 nm when the solution is cooled to room temperature (Figure 8). The electron micrograph of the cross-linked nanostructures shows aggregates with a vesicular morphology consistent with that reported in our previous work.[72] Additionally, elongated vesicular structures are observed.

Conclusions

In this work, we have described the facility by which hydrophilic-hydrophilic diblock copolymers can be synthesized and induced to undergo stimuli-responsive reorganization into nanoaggregates with specific morphology. Three DMAEMA-*b*-NIPAM copolymers with a fixed PDMAEMA length of DP = 165 and PNIPAM blocks of 102, 202, and 435 have been successfully synthesized *via* RAFT polymerization. It was shown that decreasing the hydrophobic mass fraction of the block copolymers through changes in composition, pH, or ionic strength drastically affects the resulting assembly behavior and morphology. By carefully controlling these parameters, spherical micelles, worm-like micelles, and vesicles were prepared from the stimuli-responsive, hydrophilic-hydrophilic block copolymers directly in water. Significantly, these amphiphilic diblock copolymers subjected to external stimuli behave as predicted from theory developed by Discher, Eisenberg, and others for amphiphilic diblocks with a permanently hydrophobic block. The nanostructures were subsequently cross-linked to yield AuNPs by the *in situ* reduction of $NaAuCl_4$ by the amine moieties in the PDMAEMA shells and observed by TEM. Importantly, the ability of stimuli-responsive hydrophilic-hydrophilic block copolymers to assemble directly in aqueous media provides important pathways for biologically relevant applications.

Acknowledgment. The Department of Energy (DE-FC26-01BC15317), MRSEC program of the National Science Foundation (NSF) (DMR-0213883), and the Robert M. Hearin Foundation are

gratefully acknowledged for financial support. The authors also acknowledge the NSF Division of Materials Research/Major Research Instrumentation awards 0079450 and 0421406 for the purchase of the Varian Unity Inova 500 MHz NMR spectrometer and JEOL JEM-2100 electron microscope.

Supporting Information Available: ASEC chromatograms of the $DMAEMA_{165}$ macroCTA and variable temperature ^1H NMR spectra for $DMAEMA_{165}$-*b*-$NIPAM_{435}$. This material is available free of charge via the Internet at http://pubs.acs.org.

References and Notes

(1) Becker, M. L.; Remsen, E. E.; Wooley, K. L. *J. Polym. Sci., Part A: Polym. Chem.* **2001**, *39*, 4152–4166.
(2) Butun, V.; Wang, X. S.; de PazBanez, M. V.; Robinson, K. L.; Billingham, N. C.; Armes, S. P.; Tuzar, Z. *Macromolecules* **2000**, *33*, 1–3.
(3) Fujii, S.; Cai, Y.; Weaver, J. V. M.; Armes, S. P. *J. Am. Chem. Soc.* **2005**, *127*, 7304–7305.
(4) Huang, H.; Remsen, E. E.; Wooley, K. L. *Chem. Commun.* **1998**, *1415*, 1416.
(5) Huang, H. Y.; Remsen, E. E.; Kowalewski, T.; Wooley, K. L. *J. Am. Chem. Soc.* **1999**, *121*, 3805–3806.
(6) Liu, S.; Armes, S. P. *J. Am. Chem. Soc.* **2001**, *123*, 9910–9911.
(7) Ma, Q.; Remsen, E. E.; Kowalewski, T.; Wooley, K. L. *J. Am. Chem. Soc.* **2001**, *123*, 4627–4628.
(8) Ma, Q.; Wooley, K. L. *J. Polym. Sci., Part A: Polym. Chem.* **2000**, *38*, 4805–4820.
(9) Sanji, T.; Nakatsuka, Y.; Kitayama, F.; Sakurai, H. *Chem. Commun.* **1999**, *2201*, 2202.
(10) Sanji, T.; Nakatsuka, Y.; Ohnishi, S.; Sakurai, H. *Macromolecules* **2000**, *33*, 8524–8526.
(11) Thurmond, K. B.; Kowalewski, T.; Wooley, K. L. *J. Am. Chem. Soc.* **1997**, *119*, 6656–6665.
(12) Underhill, R. S.; Liu, G. J. *Chem. Mater.* **2000**, *12*, 2082–2091.
(13) Wooley, K. L. *J. Polym. Sci., Part A: Polym. Chem.* **2000**, *38*, 1397–1407.
(14) Gohy, J. F. *Adv. Polym. Sci.* **2005**, *190*, 65–136.
(15) Jain, S.; Bates, F. S. *Science* **2003**, *300*, 460–464.
(16) Zhulina, E. B.; Adam, M.; LaRue, I.; Sheiko, S. S.; Rubinstein, M. *Macromolecules* **2005**, *38*, 5330–5351.
(17) Israelachvilli, J. N. *Intermolecular and Surface Forces*; 2nd ed.; Academic Press: San Diego, CA, 1991.
(18) Discher, D. E.; Ahmed, F. *Annu. Rev. Biomed. Eng.* **2006**, *8*, 323–341.
(19) Choucair, A.; Eisenberg, A. *Eur. Phys. J. E* **2003**, *10*, 37–44.
(20) Choucair, A.; Lavigueur, C.; Eisenberg, A. *Langmuir* **2004**, *20*, 3894–3900.
(21) Harada, A.; Kataoka, K. *Science* **1999**, *283*, 65–67.
(22) Andre, X.; Zhang, M. F.; Muller, A. H. E. *Macromol. Rapid Commun.* **2005**, *26*, 558–563.
(23) Colfen, H. *Macromol. Rapid Commun.* **2001**, *22*, 219–252.
(24) Lokitz, B. S.; Convertine, A. J.; Ezell, R. G.; Heidenreich, A.; Li, Y.; McCormick, C. L. *Macromolecules* **2006**, *39*, 8594–8602.
(25) Riess, G. *Prog. Polym. Sci.* **2003**, *28*, 1107–1170.
(26) Rodriguez-Hernandez, J.; Babin, J.; Zappone, B.; Lecommandoux, S. *Biomacromolecules* **2005**, *6*, 2213–2220.
(27) Rodriguez-Hernandez, J.; Checot, F.; Gnanou, Y.; Lecommandoux, S. *Prog. Polym. Sci.* **2005**, *30*, 691–724.
(28) Butun, V.; Liu, S.; Weaver, J. V. M.; Bories-Azeau, X.; Cai, Y.; Armes, S. P. *React. Funct. Polym.* **2006**, *66*, 157–165.
(29) Liu, F.; Eisenberg, A. *J. Am. Chem. Soc.* **2003**, *125*, 15059–15064.
(30) Liu, S. Y.; Armes, S. P. *Angew. Chem., Int. Ed.* **2002**, *41*, 1413–1416.
(31) Xu, C.; Wayland, B. B.; Fryd, M.; Winey, K. I.; Composto, R. J. *Macromolecules* **2006**, *39*, 6063–6070.
(32) Aubrecht, K. B.; Grubbs, R. B. *J. Polym. Sci., Part A: Polym. Chem.* **2005**, *43*, 5156–5167.
(33) Hay, D. N. T.; Rickert, P. G.; Seifert, S.; Firestone, M. A. *J. Am. Chem. Soc.* **2004**, *126*, 2290–2291.
(34) Sundararaman, A.; Stephan, T.; Grubbs, R. B. *J. Am. Chem. Soc.* **2008**, *130*, 12264–12265.
(35) Dimitrov, I.; Trzebicka, B.; Mueller, A. H. E.; Dworak, A.; Tsvetanov, C. B. *Prog. Polym. Sci.* **2007**, *32*, 1275–1343.
(36) Liu, S.; Billingham, N. C.; Armes, S. P. *Angew. Chem., Int. Ed.* **2001**, *40*, 2328–2331.
(37) Schilli, C. M.; Zhang, M.; Rizzardo, E.; Thang, S. H.; Chong, Y. K.; Edwards, K.; Karlsson, G.; Mueller, A. H. E. *Macromolecules* **2004**, *37*, 7861–7866.
(38) Nuopponen, M.; Tenhu, H. *Langmuir* **2007**, *23*, 5352–5357.
(39) Amalvy, J. I.; Unali, G. F.; Li, Y.; Granger-Bevan, S.; Armes, S. P.; Binks, B. P.; Rodrigues, J. A.; Whitby, C. P. *Langmuir* **2004**, *20*, 4345–4354.
(40) Mueller, K. H. *Polymer* **1992**, *33*, 3470–3476.
(41) Yuk, S. H.; Cho, S. H.; Lee, S. H. *Macromolecules* **1997**, *30*, 6856–6859.
(42) Kwon, G. S.; Okano, T. *Adv. Drug Delivery Rev.* **1996**, *21*, 107–116.
(43) Hales, M.; Barner-Kowolik, C.; Davis, T. P.; Stenzel, M. H. *Langmuir* **2004**, *20*, 10809–10817.
(44) Thurmond, K. B.; Kowalewski, T.; Wooley, K. L. *J. Am. Chem. Soc.* **1996**, *118*, 7239–7240.
(45) Huang, H. Y.; Kowalewski, T.; Remsen, E. E.; Gertzmann, R.; Wooley, K. L. *J. Am. Chem. Soc.* **1997**, *119*, 11653–11659.
(46) Remsen, E. E.; Thurmond, K. B.; Wooley, K. L. *Macromolecules* **1999**, *32*, 3685–3689.
(47) Zhang, Q.; Remsen, E. E.; Wooley, K. L. *J. Am. Chem. Soc.* **2000**, *122*, 3642–3651.
(48) Butun, V.; Billingham, N. C.; Armes, S. P. *J. Am. Chem. Soc.* **1998**, *120*, 11818–11819.
(49) Butun, V.; Lowe, A. B.; Billingham, N. C.; Armes, S. P. *J. Am. Chem. Soc.* **1999**, *121*, 4288–4289.
(50) Liu, S. Y.; Weaver, J. V. M.; Tang, Y. Q.; Billingham, N. C.; Armes, S. P.; Tribe, K. *Macromolecules* **2002**, *35*, 6121–6131.
(51) Liu, S. Y.; Ma, Y. H.; Armes, S. P. *Langmuir* **2002**, *18*, 7780–7784.
(52) Li, Y.; Lokitz, B. S.; McCormick, C. L. *Angew. Chem., Int. Ed.* **2006**, *45*, 5792–5795.
(53) Weaver, J. V. M.; Tang, Y.; Liu, S.; Iddon, P. D.; Grigg, R.; Armes, S. P.; Billingham, N. C.; Hunter, R.; Rannard, S. P. *Angew. Chem., Int. Ed.* **2004**, *43*, 1389–1392.
(54) Lokitz, B. S.; York, A. W.; Stempka, J. E.; Treat, N. D.; Li, Y.; Jarrett, W. L.; McCormick, C. L. *Macromolecules* **2007**, *40*, 6473–6480.
(55) Matsumoto, K.; Hirabayashi, T.; Harada, T.; Matsuoka, H. *Macromolecules* **2005**, *38*, 9957–9962.
(56) Joralemon, M. J.; O'Reilly, R. K.; Hawker, C. J.; Wooley, K. L. *J. Am. Chem. Soc.* **2005**, *127*, 16892–16899.
(57) Li, Y.; Lokitz, B. S.; Armes, S. P.; McCormick, C. L. *Macromolecules* **2006**, *39*, 2726–2728.
(58) Li, Y.; Lokitz, B. S.; McCormick, C. L. *Macromolecules* **2006**, *39*, 81–89.
(59) Read, E. S.; Armes, S. P. *Chem. Commun.* **2007**, *3021*, 3035.
(60) Daniel, M.-C.; Astruc, D. *Chem. Rev.* **2004**, *104*, 293–346.
(61) Brust, M.; Walker, M.; Bethell, D.; Schiffrin, D. J.; Whyman, R. *J. Chem. Soc., Chem. Commun.* **1994**, *801*, 802.
(62) Lowe, A. B.; Sumerlin, B. S.; Donovan, M. S.; McCormack, C. L. *J. Am. Chem. Soc.* **2002**, *124*, 1152–11563.
(63) Shan, J.; Nuopponen, M.; Jiang, H.; Viitala, T.; Kauppinen, E.; Kontturi, K.; Tenhu, H. *Macromolecules* **2005**, *38*, 2918–2926.
(64) Yuan, J.-J.; Schmid, A.; Armes, S. P. *Langmuir* **2006**, *22*, 11022–11027.
(65) Mirkin, C. A.; Letsinger, R. L.; Mucic, R. C.; Storhoff, J. J. *Nature* **1996**, *382*, 607–609.
(66) Li, Z.; Jin, R.; Mirkin, C. A.; Letsinger, R. L. *Nucleic Acids Res.* **2002**, *30*, 1558–1562.
(67) Alivisatos, A. P.; Johnsson, K. P.; Peng, X.; Wilson, T. E.; Loweth, C. J.; Bruchez, M. P. J.; Schultz, P. G. *Nature* **1996**, *382*, 609–611.
(68) Bronstein, L. M.; Sidorov, S. N.; Gourkova, A. Y.; Valetsky, P. M.; Hartmann, J.; Breulmann, M.; Colfen, H.; Antonietti, M. *Inorg. Chim. Acta* **1998**, *280*, 348–354.
(69) Yu, S. H.; Colfen, H.; Mastai, Y. *J. Nanosci. Nanotechnol.* **2004**, *4*, 291–298.
(70) Sun, X.; Dong, S.; Wang, E. *Mater. Chem. Phys.* **2006**, *96*, 29–33.
(71) Ishii, T.; Otsuka, H.; Kataoka, K.; Nagasaki, Y. *Langmuir* **2004**, *20*, 561–564.
(72) Li, Y.; Smith, A. E.; Lokitz, B. S.; McCormick, C. L. *Macromolecules* **2007**, *40*, 8524–8526.
(73) Lowe, A. B.; McCormick, C. L. *Prog. Polym. Sci.* **2007**, *32*, 283–351.
(74) Moad, G.; Rizzardo, E.; Thang, S. H. *Aust. J. Chem.* **2005**, *58*, 379–410.
(75) Perrier, S.; Takolpuckdee, P. *J. Polym. Sci., Part A: Polym. Chem.* **2005**, *43*, 5347–5393.
(76) McCormick, C. L.; Lowe, A. B. *Acc. Chem. Res.* **2004**, *37*, 312–325.
(77) Mitsukami, Y.; Donovan, M. S.; Lowe, A. B.; McCormick, C. L. *Macromolecules* **2001**, *34*, 2248–2256.
(78) De, P.; Gondi, S. R.; Sumerlin, B. S. *Macromolecules* **2008**, *9*, 1064–1070.
(79) Convertine, A. J.; Lokitz, B. S.; Vasileva, Y.; Myrick, L. J.; Scales, C. W.; Lowe, A. B.; McCormick, C. L. *Macromolecules* **2006**, *39*, 1724–1730.

MA802827P